catalysts

MDPI

*Supporting Information*

# Influence of Dopants on Pt/$Al_2O_3$-Based Monolithic Catalysts for Autothermal Oxidative Coupling of Methane

**Sven Schardt, Simon Bastian, Ahmet Çelik, Jaspreet Chawla and Patrick Lott ***

Institute for Chemical Technology and Polymer Chemistry (ITCP), Karlsruhe Institute of Technology (KIT), 76131 Karlsruhe, Germany; sven.schardt@kit.edu (S.S.); simon.bastian@kit.edu (S.B.); ahmet.celik@kit.edu (A.Ç.); jaspreet.chawla@kit.edu (J.C.)
* Correspondence: patrick.lott@kit.edu

**Abstract:** Autothermal oxidative coupling of methane (OCM) is a highly attractive approach for methane utilization. If platinum-based catalysts are operated in short-contact-time reactors with high space velocities, high methane conversion can be achieved. Using a 1 wt.% Pt/$Al_2O_3$ catalyst as a benchmark, the present study elucidates how different dopants, namely Ni, Sn, and $V_2O_5$, affect the OCM reaction. Kinetic catalyst tests reveal that acetylene ($C_2H_2$) is the predominant $C_2$ product, irrespective of the catalyst formulation or operation conditions. Furthermore, the use of bimetallic catalysts allows either for the maintenance or even the improvement of the $C_2$ selectivity during OCM, which is attributed to synergistic effects that occur when expensive Pt is partially replaced by cheaper dopants. In particular, the 1 wt.% Pt/$Al_2O_3$ reference catalyst yielded a maximum $C_2$ selectivity of 8.2%, whereas the best-performing doped sample 0.25 wt.% Pt 0.75 wt.% $V_2O_5$/$Al_2O_3$ yielded a total $C_2$ selectivity of 11.3%.

**Keywords:** oxidative coupling of methane; doping; heterogeneous catalysis; gas-phase reactions; methane upgrading

## 1. Definition of Conversion, Yield, and Selectivity

Equations S1–S5 give the definitions of the methane conversion (Equation S1), product yields (Equations S2 and S3), and the product selectivity (Equations S4 and S5) as used within this study.

$$X_{CH_4} = \frac{\dot{n}_{CH_4,out}}{\dot{n}_{CH_4,in}} \quad (S1)$$

$$Y_{CO} = \frac{\dot{n}_{CO,out} - \dot{n}_{CO,in}}{\dot{n}_{CH_4,in}} \quad (S2)$$

$$Y_{C_2H_2} = \frac{2 \cdot (\dot{n}_{C_2H_2,out} - \dot{n}_{C_2H_2,in})}{\dot{n}_{CH_4,in}} \quad (S3)$$

$$S_{CO} = \frac{\dot{n}_{CO,out} - \dot{n}_{CO,in}}{\dot{n}_{CH_4,in} - \dot{n}_{CH_4,out}} \quad (S4)$$

$$S_{C_2H_2} = \frac{2 \cdot (\dot{n}_{C_2H_2,out} - \dot{n}_{C_2H_2,in})}{\dot{n}_{CH_4,in} - \dot{n}_{CH_4,out}} \quad (S5)$$

Figure S1 shows the total $C_2$ yield as well as the yield for the three $C_2$ species $C_2H_6$, $C_2H_4$, and $C_2H_2$ and the temperature measured downstream of the catalyst versus the nitrogen dilution in the feed for the 1 wt.% Pt/$Al_2O_3$ catalyst at both investigated space velocities of 458,000 $h^{-1}$ (Figure S1A) and 295,000 $h^{-1}$ (Figure S1B). For the reference dilution value of 50 vol.% $N_2$ in the feed, all product selectivities and methane conversion values are given in Table S1 (458,000 $h^{-1}$) and Table S2 (295,000 $h^{-1}$). Please note that the hydrogen content in the effluent gas stream was not directly measured but instead calculated via the hydrogen balance.

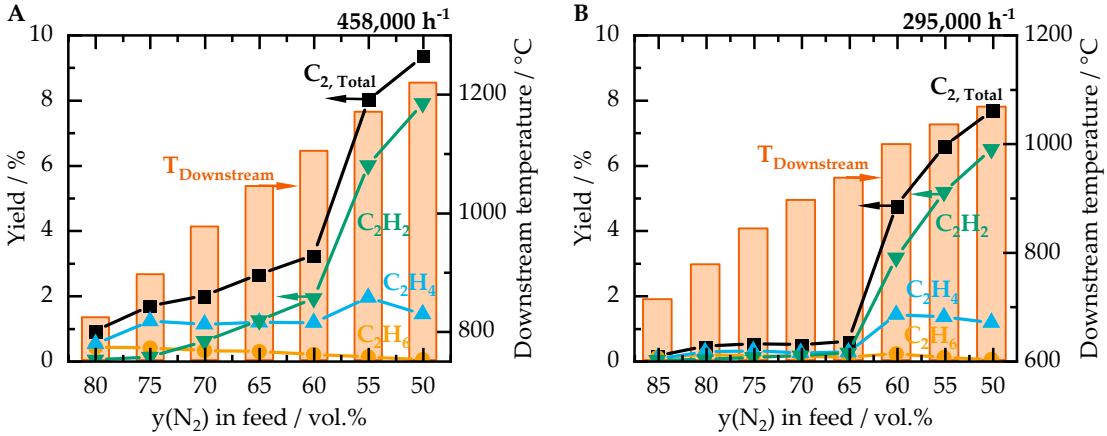


**Figure S1.** Yield and downstream temperature versus the $N_2$ content in the feed of the 1 wt.% $Pt/Al_2O_3$ catalyst for (**A**) a GHSV of 458,000 $h^{-1}$ and (**B**) a GHSV of 295,000 $h^{-1}$.

**Table S1.** Methane conversion and product selectivities for all catalysts tested at a GHSV of 458,000 $h^{-1}$, a nitrogen content of 50% in the feed, and a C:O ratio of 0.55. Please note that the hydrogen content in the effluent gas stream was not directly measured but instead calculated via the hydrogen balance. Total active material loading of 1 wt.% for all bimetallic samples.

| Catalyst | X($CH_4$) | S($C_2H_2$) | S($C_2H_4$) | S($C_2H_6$) | S(CO) | S($CO_2$) | S($H_2O$) | S($H_2$) |
|---|---|---|---|---|---|---|---|---|
| 1 wt.% $Pt/Al_2O_3$ | 90.6% | 8.7% | 1.6% | 0.0% | 65.8% | 0.4% | 43.8% | 53.2% |
| 0.5 wt.% $Pt/Al_2O_3$ | 91.9% | 7.8% | 1.2% | 0.0% | 67.0% | 1.2% | 40.9% | 56.5% |
| Pt-$V_2O_5$ (3:1) | 88.8% | 8.2% | 2.4% | 0.0% | 65.0% | 1.9% | 45.7% | 51.0% |
| Pt-$V_2O_5$ (1:3) | 84.5% | 7.3% | 3.0% | 0.2% | 64.6% | 6.6% | 51.0% | 45.5% |
| Pt-Sn (3:1) | 85.9% | 7.4% | 2.9% | 0.2% | 66.3% | 5.9% | 49.9% | 46.7% |
| Pt-Sn (1:3) | 84.6% | 6.9% | 3.1% | 0.3% | 66.2% | 6.3% | 50.9% | 45.6% |
| Pt-Ni (3:1) | 91.0% | 8.6% | 1.6% | 0.0% | 65.3% | 3.2% | 43.2% | 53.8% |
| Pt-Ni (1:3) | 88.3% | 8.7% | 2.3% | 0.0% | 63.6% | 2.3% | 46.6% | 50.0% |

**Table S2.** Methane conversion and product selectivities for all catalysts tested at a GHSV of 295,000 $h^{-1}$, a nitrogen content of 50% in the feed, and a C:O ratio of 0.55. Please note that the hydrogen content in the effluent gas stream was not directly measured but instead calculated via the hydrogen balance; although the ethane selectivity was below 0.05% for all catalyst formulations subject to this study, it was still considered for calculating the total $C_2$ selectivity, e.g., resulting in a total $C_2$ selectivity of 11.3% for Pt-$V_2O_5$ (1:3). Total active material loading of 1 wt.% for all bimetallic samples.

| Catalyst | X($CH_4$) | S($C_2H_2$) | S($C_2H_4$) | S($C_2H_6$) | S(CO) | S($CO_2$) | S($H_2O$) | S($H_2$) |
|---|---|---|---|---|---|---|---|---|
| 1 wt.% Pt/$Al_2O_3$ | 92.2% | 7.0% | 1.2% | 0.0% | 66.6% | 2.0% | 39.7% | 57.9% |
| 0.5 wt.% Pt/$Al_2O_3$ | 92.6% | 6.4% | 1.2% | 0.0% | 66.6% | 4.7% | 38.6% | 59.1% |
| Pt-$V_2O_5$ (1:3) | 89.1% | 9.2% | 2.0% | 0.0% | 59.4% | 4.1% | 46.0% | 50.6% |
| Pt-Sn (1:3) | 89.4% | 9.1% | 1.5% | 0.0% | 61.4% | 4.1% | 46.5% | 50.5% |
| Pt-Ni (1:3) | 90.8% | 8.5% | 1.6% | 0.0% | 61.4% | 0.4% | 42.6% | 54.5% |

## 2. Structural Analysis

The elemental analysis results are summarized in Table S3 and confirm the target metal loading(s). Figure S2 shows a comparison of the results of the elemental analysis for both fresh and spent samples. Please note that the sample for 1 wt.% Pt/$Al_2O_3$ could not be analyzed due to a human error during sample processing. Table S4 summarizes the $N_2$ physisorption measurement results. All samples are within the same range considering the surface area, and only Pt-$V_2O_3$ (3:1) shows a lower pore volume than all other catalysts. Since this specific catalyst did not show exceptional results and all others are almost identical, we considered the effect of the structural parameters on the catalytic activity negligible for our materials subject to our study.

**Table S3.** Results from the ICP-OES elemental analysis for the catalysts. The dopant content refers to the respective doped metal, if applicable.

| Catalytic system | Pt content / % | Dopant content / % | Al content / % |
|---|---|---|---|
| 1 wt.% Pt/$Al_2O_3$ | 0.998 | n.a. | 48.1 |
| 0.5 wt.% Pt/$Al_2O_3$ | 0.445 | n.a. | 45.5 |
| Pt-$V_2O_5$ (3:1) | 0.725 | 0.152 | 49.1 |
| Pt-$V_2O_5$ (1:3) | 0.271 | 0.446 | 47.9 |
| Pt-Sn (3:1) | 0.719 | 0.294 | 48.8 |
| Pt-Sn (1:3) | 0.278 | 0.748 | 47.3 |
| Pt-Ni (3:1) | 0.734 | 0.272 | 48.9 |
| Pt-Ni (1:3) | 0.265 | 0.754 | 47.0 |

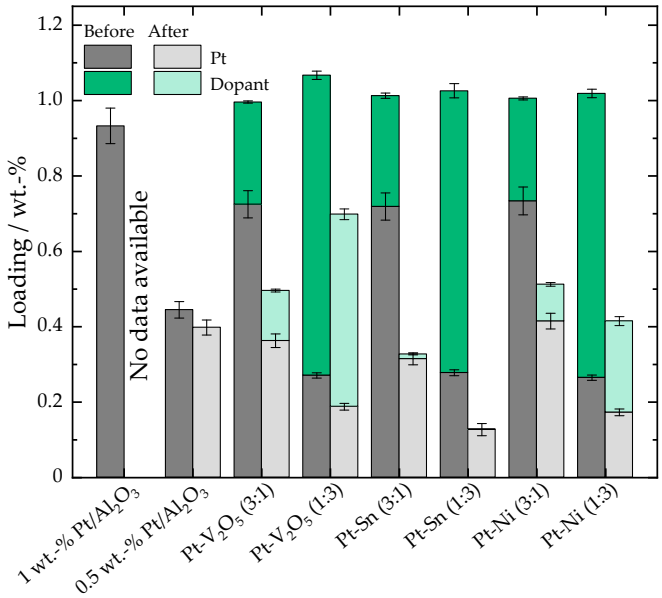


**Figure S2.** Comparison of the elemental analysis results for the catalysts before (left bar, darker color) and after (right bar, lighter color) usage with the Pt content in grey and the respective dopant content in green. Please note that for reasons of clarity, the oxygen content for the $V_2O_5$ species was added and that the processing of the 1 wt.% $Pt/Al_2O_3$ sample was faulty, therefore resulting in no usable data.

**Table S4.** Results of the $N_2$ physisorption experiments. Both surface area and pore volume are determined with the BET method. Total active material loading of 1 wt.% for all bimetallic samples.

| Catalytic system | Surface area / $m^2\ g^{-1}$ | Pore volume / $cm^3(STP)\ g^{-1}$ |
|---|---|---|
| Calcined $\gamma$-$Al_2O_3$ | 210 | 0.50 |
| 1 wt.% $Pt/Al_2O_3$ | 204 | 0.49 |
| 0.5 wt.% $Pt/Al_2O_3$ | 211 | 0.50 |
| Pt-$V_2O_5$ (3:1) | 203 | 0.38 |
| Pt-$V_2O_5$ (1:3) | 204 | 0.48 |
| Pt-Sn (3:1) | 202 | 0.48 |
| Pt-Sn (1:3) | 215 | 0.49 |
| Pt-Ni (3:1) | 201 | 0.50 |
| Pt-Ni (1:3) | 205 | 0.49 |

### 3. Absolute Values for Measurements at 458,000 $h^{-1}$ and 295,000 $h^{-1}$

For better comparability, the absolute concentrations for the measurements at 458,000 $h^{-1}$ and 295,000 $h^{-1}$ at 50% dilution and a C:O ratio of 0.55 gathered by means of FTIR spectroscopy are given in Table S5 and Table S6, respectively. Due to the typically high $C_2$ contents in the gas stream, which would exceed the calibration levels of the FTIR (MG2030, MKS Instruments), the volume flow entering the FTIR is diluted with nitrogen and increased by about 60% from 6 slpm to almost 10 slpm for the measurements at 458,000 $h^{-1}$ and doubled from 3.9 slpm to 7.8 slpm for the measurements at 295,000 $h^{-1}$. The reason for the difference in added diluent is the maximum total flow that was possible inside the exhaust pipes of the setup without causing a significant backpressure. Please note that the NO concentration results from the tracing system in our reactor are described in more detail in the experimental section of the main manuscript.

**Table S5.** Absolute concentrations of the $C_2$ species determined by means of FTIR at a GHSV of 458,000 $h^{-1}$, a nitrogen content of 50% in the feed, and a C:O ratio of 0.55. Total active material loading of 1 wt.% for all bimetallic samples. Please note that the volume flow entering the FTIR is increased compared to the reactor exit flow rate due to a further dilution of the exhaust gas prior to the analytics.

| Catalyst | c($CH_4$) / % | c($C_2H_2$) / ppm | c($C_2H_4$) / ppm | c($C_2H_6$) / ppm | c(CO) / % | c($CO_2$) / % | c($H_2O$) / % | c($C_3H_6$) / ppm | c(NO) / ppm | $V_{total}$ / slpm |
|---|---|---|---|---|---|---|---|---|---|---|
| 1 wt.% Pt | 1.48 | 6252 | 1122 | 9 | 9.42 | 0.06 | 12.56 | 15 | 139 | 9.94 |
| 0.5 wt.% Pt | 1.28 | 5667 | 906 | 4 | 9.73 | 0.17 | 11.89 | 10 | 140 | 9.94 |
| Pt-$V_2O_5$ (3:1) | 1.78 | 5753 | 1684 | 43 | 9.13 | 0.27 | 12.82 | 25 | 139 | 9.94 |
| Pt-$V_2O_5$ (1:3) | 2.45 | 4886 | 1980 | 149 | 8.63 | 0.88 | 13.63 | 45 | 143 | 9.94 |
| Pt-Sn (3:1) | 2.19 | 5191 | 1910 | 122 | 9.04 | 0.78 | 13.57 | 40 | 141 | 9.94 |
| Pt-Sn (1:3) | 2.43 | 4612 | 2062 | 191 | 8.85 | 0.85 | 13.62 | 46 | 143 | 9.94 |
| Pt-Ni (3:1) | 1.44 | 6196 | 1172 | 16 | 9.37 | 0.46 | 12.41 | 14 | 139 | 9.94 |
| Pt-Ni (1:3) | 1.85 | 6096 | 1633 | 28 | 8.87 | 0.32 | 13.00 | 27 | 140 | 9.94 |

**Table S6.** Absolute concentrations of the $C_2$ species determined by means of FTIR at a GHSV of 295,000 $h^{-1}$, a nitrogen content of 50% in the feed, and a C:O ratio of 0.55. Total active material loading of 1 wt.% for all bimetallic samples. Please note that the volume flow entering the FTIR is increased compared to the reactor exit flow rate due to a further dilution of the exhaust gas prior to the analytics.

| Catalyst | c($CH_4$) / % | c($C_2H_2$) / ppm | c($C_2H_4$) / ppm | c($C_2H_6$) / ppm | c(CO) / % | c($CO_2$) / % | c($H_2O$) / % | c($C_3H_6$) / ppm | c(NO) / ppm | $V_{total}$ / slpm |
|---|---|---|---|---|---|---|---|---|---|---|
| 1 wt.% Pt | 1.01 | 4205 | 743 | 14 | 7.95 | 0.24 | 9.48 | 8 | 179 | 7.80 |
| 0.5 wt.% Pt | 0.96 | 3843 | 742 | 21 | 7.99 | 0.57 | 9.26 | 7 | 180 | 7.80 |
| Pt-$V_2O_5$ (1:3) | 1.42 | 5403 | 1176 | 29 | 6.95 | 0.48 | 10.77 | 24 | 179 | 7.80 |
| Pt-Sn (1:3) | 1.38 | 5256 | 842 | 7 | 7.11 | 0.47 | 10.78 | 15 | 181 | 7.80 |
| Pt-Ni (1:3) | 1.19 | 5009 | 938 | 14 | 7.22 | 0.05 | 10.02 | 15 | 179 | 7.80 |

**Disclaimer/Publisher's Note:** The statements, opinions and data contained in all publications are solely those of the individual author(s) and contributor(s) and not of MDPI and/or the editor(s). MDPI and/or the editor(s) disclaim responsibility for any injury to people or property resulting from any ideas, methods, instructions or products referred to in the content.